

**Zeitschrift:** IABSE congress report = Rapport du congrès AIPC = IVBH  
Kongressbericht

**Band:** 12 (1984)

**Rubrik:** Last minute's reports

### **Nutzungsbedingungen**

Die ETH-Bibliothek ist die Anbieterin der digitalisierten Zeitschriften. Sie besitzt keine Urheberrechte an den Zeitschriften und ist nicht verantwortlich für deren Inhalte. Die Rechte liegen in der Regel bei den Herausgebern beziehungsweise den externen Rechteinhabern. [Siehe Rechtliche Hinweise.](#)

### **Conditions d'utilisation**

L'ETH Library est le fournisseur des revues numérisées. Elle ne détient aucun droit d'auteur sur les revues et n'est pas responsable de leur contenu. En règle générale, les droits sont détenus par les éditeurs ou les détenteurs de droits externes. [Voir Informations légales.](#)

### **Terms of use**

The ETH Library is the provider of the digitised journals. It does not own any copyrights to the journals and is not responsible for their content. The rights usually lie with the publishers or the external rights holders. [See Legal notice.](#)

**Download PDF:** 15.03.2025

**ETH-Bibliothek Zürich, E-Periodica, <https://www.e-periodica.ch>**



## **Last Minute's Reports**

Leere Seite  
Blank page  
Page vide

## Cable Stayed Bridges – Developments and Perspective

Ponts à haubans – Développements et perspectives d'avenir

Seilverspannte Betonbrücken – Entwicklung und Zukunft

### Jean MULLER

Chairman of Board  
Figg and Muller Engineers Inc.  
Courbevoie, France



Jean Muller received his Bachelors in Mathematics in 1943 and his Masters Degree in Civil Engineering from the Ecole Centrale des Arts et Manufactures, Paris, in 1947. He then worked for Freyssinet International, Paris, and was the Chief Engineer for Freyssinet Company, New York. From 1955 to 1976 Jean Muller worked for Campenon Bernard, Paris. Figg and Muller Engineers, Inc., of which he is Chairman of the Board and Partner in Charge of all Technical Design, was formed in 1978.

### SUMMARY

Concrete cable stayed bridges were increasingly used for the last ten years in span ranges of 250 to 350 m. With existing materials and technology, span of 400 to 450 m can be crossed easily. For longer spans, steel and concrete should be used in composite structures. However, the most characteristic progress was accomplished in moderate span length, thanks to the three following items: choice of cross section in relation with aeroelastic stability; simplification of suspension system and stay anchors; use of existing and simple construction techniques already proven on conventional bridges. Important savings may be obtained through the use of cable stayed concrete bridges with spans of 150 to 200 m over conventional box-girder bridges.

### RESUME

Les ponts à haubans en béton se sont développés rapidement depuis dix ans dans le domaine des grandes portées de 250 à 350 mètres. Avec les matériaux et la technologie actuels, on peut franchir sans problème des portées de 400 à 450 mètres. Au delà, il faut associer le béton et la charpente métallique dans des structures mixtes. Les progrès les plus caractéristiques ont, cependant, été accomplis dans les portées grâce aux trois éléments suivants: choix de la section transversale en fonction des efforts aéroélastiques; simplification dans la suspension et la réalisation des ancrages des haubans; utilisation de méthodes de construction simples et déjà éprouvées pour des ponts traditionnels. Des économies importantes sont possibles par l'utilisation de ponts haubannés dans des portées de 150 à 200 mètres, par rapport aux solutions traditionnelles de ponts à poutres en caissons.

### ZUSAMMENFASSUNG

In den letzten zehn Jahren nahm die Anzahl seilvorgespannter Betonbrücken mit Spannweiten von 250 m bis 300 m zu. Brücken aus bestehenden Materialien und Technologien überspannen ohne Schwierigkeiten 400 bis 450 m. Die Verbundbauweise mit Stahl und Beton ermöglicht sogar noch grössere Spannweiten. Trotzdem, diese Bauweise fand hauptsächlich bei Brücken mit mittleren Spannweiten ihre Anwendung. Die folgenden drei Gründe haben dazu beigetragen: Wahl des Querschnittes unter Berücksichtigung der Stabilität für Windbeanspruchung; Vereinfachung des Aufhängesystems und der Verankerung; Verwendung von bestehenden und einfachen Konstruktionstechniken, deren Zweckmässigkeit im konventionellen Brückenbau bereits ausgetestet ist. Die seilverspannten Betonbrücken sind vor allem in Spannweitenbereichen von 150 m bis 200 m den konventionellen Kasten-trägerbrücken vom wirtschaftlichen Standpunkt aus gesehen, überlegen.



## 1. HISTORICAL BACKGROUND

The first modern long span cable stayed bridge was proposed by Eugene Freyssinet in 1952 for crossing of the Seine River at Tancarville. The 2000 ft long main clear span was supported by multiple stays anchored in two short side spans with the contribution of outside anchorage structures to relieve the deck from excessive compressive stresses induced by the longitudinal components of the stay loads.

Tancarville bridge was finally built as a conventional suspension bridge and Freyssinet's scheme was only an anticipation of future developments.

## 2. BROTONNE BRIDGE, FRANCE

Twenty five years later, Brotonne Bridge was opened to traffic. With a more modest span of 1050 ft over the same river - just 30 miles upstream of Tancarville - it still represents to-day the longest concrete cable stayed bridge before completion of the Sunshine Skyway Bridge in Tampa, Florida now under construction with a main clear span of 1200 ft. Between the conception of these two projects, Tancarville and Brotonne, precast segmental construction with match marking joints was developed and its potential was made available for design and construction of long span concrete cable stayed bridges.

Brotonne Bridge's salient features are:

2.1. The deck is made of a single box with internal stiffeners suspended on a single plane of stays and single concrete pylons. The safety of this scheme may be made as large as desired by proper choice of pylon dimensions and magnitude of reinforcement. In the case of Brotonne Bridge, the wind pressure causing instability would be in excess of 130 psf.

2.2. The deck of the main crossing is continuous over the transition piers with the approach spans while a moment transfer connection is provided between deck, pylon and main pier. This special static scheme greatly reduces the variation of live load moments in the deck which allowing cantilever construction of the main river span without temporary towers or strengthening devices.

2.3. Stays consist of prestressing strands encased in a steel pipe and pressure grouted after stressing. End anchorages in the deck are an extrapolation of conventional post tensioning hardware with provisions for future stay load adjustments. Each stay is continuous through the concrete pylon with an embedded sleeve pipe. The effect of bending stresses in the stays resulting from the change of sag and the deck deflections are minimized through the use of a thick pipe section near the pylons and the deck.

Damping devices are provided at deck level to control vibration.

The stays were installed without scaffolding with the help of rolling chairs similar to those of a ski lift.

After seven years of operation, Brotonne Bridge has shown to perform very satisfactorily. This year (1984) the stays were readjusted to compensate for all long term concrete strains and it is not anticipated that any further adjustment will ever be required. (see the finished bridge by night fig. 5)

## 3. COATZACOALCOS BRIDGE, MEXICO

A concept similar to Brotonne Bridge is applied to the construction of Coatzacoalcos Bridge in Mexico. With dimensions comparable to Brotonne Bridge (main span length is



945 ft and deck width is 59 ft), the cast-in-place deck is suspended on a single centerplane of stays which in turn transfers the deck load to the main delta framed pylons. The description of this interesting structure and its related developments are reported by others in this Congress.

#### 4. A NEW PROPOSED PYLON AND STAY SCHEME FOR MOONEY MOONEY CREEK BRIDGE, AUSTRALIA

Brotonne Bridge features single center pylons supporting a single plane of stays.

Coatzacoalcos Bridge features in fact a single plane of stays and a double pylon system.

When the author was asked in 1980 to review the design of the Mooney Mooney Creek Bridge in Australia for the Department of Main Roads of New South Wales, a new challenge had to be met. Substantial mining subsidence effects had to be considered while the deck width of 100 ft to accommodate six lanes of traffic was substantially wider than of previous references. The scheme proposed for this concrete cable stayed bridge was based on the following options: (Fig 1.)

- A torsionally resistant deck section with a curved intrados and transverse webs at 20 ft intervals, the same interval as the stays.
- Single pylons placed at the deck centerline supporting two families of radiating stays located in two inclined planes.

This scheme was found to be efficient to insure the elastic stability of the pylon and stay system while minimizing the harmful effects of differential settlements of the foundations.

In spite of its attractiveness, this project was not built because cost studies had shown that for that particular site where no restrictions were imposed on the location and number of piers, a conventional box girder design was more economical, at the time.

#### 5. CONCRETE CABLE STAYED BRIDGES IN THE UNITED STATES - PREVIOUS EXPERIENCE WITH SEGMENTAL CONSTRUCTION

Today the largest concrete cable stayed bridge in North America is the Pasco Kennewick Bridge in the State of Washington, designed by Pr Leonhardt and Arvid Grant and built by Peter Kiewit and Sons Co. with a main span of 980 ft.

The new Sunshine Skyway Bridge (presently under construction over Tampa Bay, Florida), incorporates many new developments in the field of precast segmental construction. It is therefore of interest to briefly review the experience gained in that field since the design of the Florida Keys Bridges. Several new items were introduced at this occasion:

- Pretensioning of the roadway slab.
- Assembly of precast segments on a truss in complete continuous spans.
- Longitudinal post tensioning created by tendons located inside the box girder but outside the concrete walls of the section. Such tendons are placed inside polyethylene ducts and pressure grouted after stressing. Proper overlapping of the tendons of each span over the successive piers achieves full continuity for all loads over several spans on a total length of about 1000 ft.
- Riding on the as-cast surface with no waterproof membrane or/and pavement.
- Dry joints between match marked segments are used with no epoxy.

After the successful experience of the four segmental bridges in the Florida Keys which represent a total deck area in excess of 2,200,000 SF, several other structures were designed and successfully built.

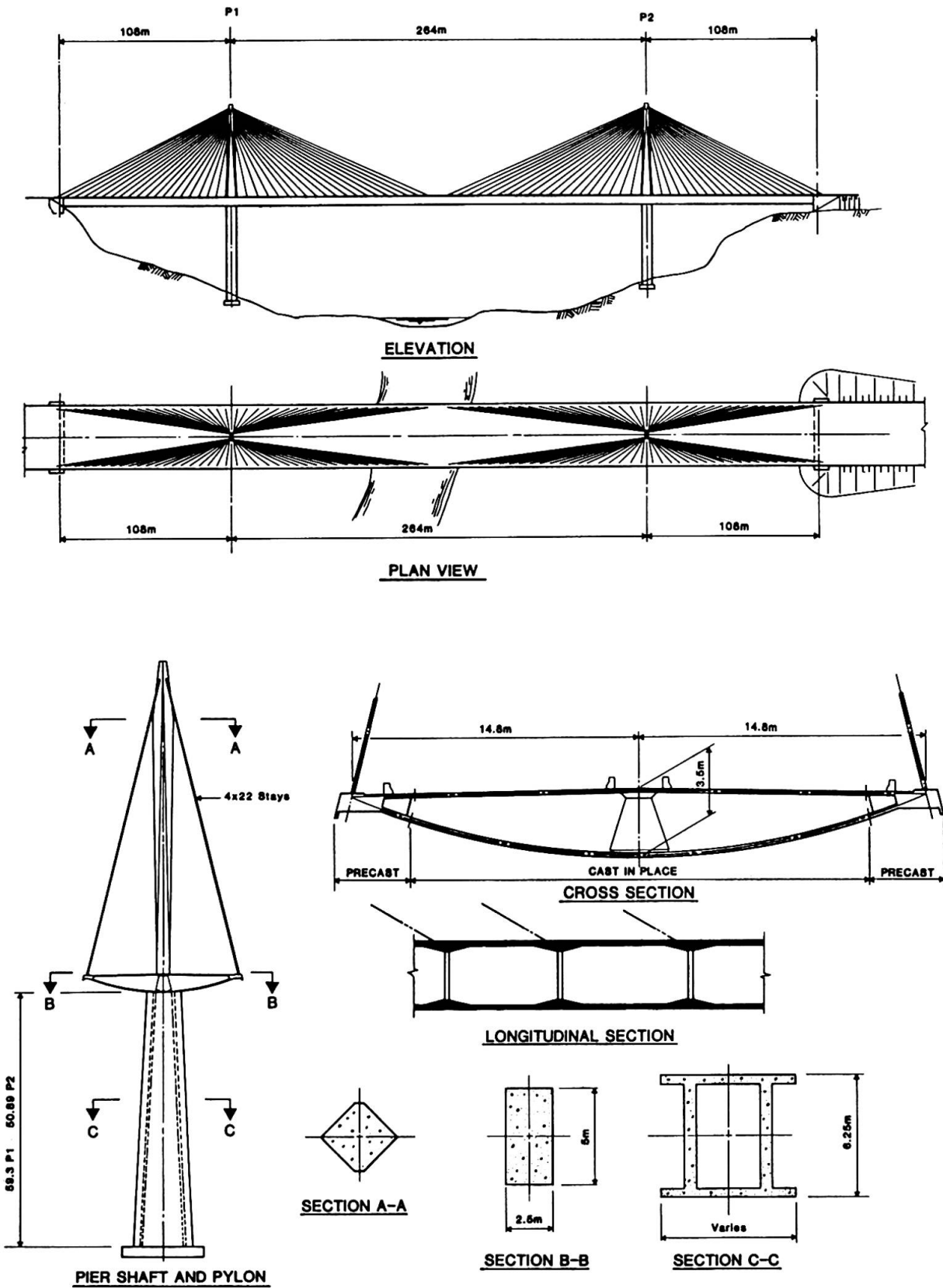


FIG. 1. PROPOSED CONCEPT FOR MOONEY MOONEY CREEK BRIDGE

Of particular interest are:

- Wiscasset Bridge, Maine.

Climatic conditions dictated the use of epoxy in the joints and of both a waterproof membrane and a bituminous pavement over the concrete deck slab.

Dauphin Island Bridge, Alabama.

With a 400 ft main span built of precast segmental construction. The contractor accepted the challenge of building this main span to stringent specifications to allow riding on the as-cast surface as was specified for the approach spans. The result has been very satisfactory.

- Linn Cove Viaduct, North Carolina.

Of moderate dimensions only, this structure symbolizes however the utmost geometric complications with the most stringent environmental constraints. All construction proceeded from the deck with the exception of minor foundation work and the use of precast segmental construction has proven capable of fully meeting this challenge.

- Mark Clark Expressway in Charleston, South Carolina.

With a construction budget of 250 million US dollars, this large project implies several structures of unusual interest:

- a precast cable stayed crossing with a clear span of 800 ft over Cooper River,

- a precast box girder bridge with a clear span of 400 ft over the Wando River,

- difficult foundation conditions over a waste disposal area,

- urban interchanges,

all structures being located in a seismically active zone.

To ascertain the suitability of our concepts of precast segmental construction with external tendons to sustain seismic loads, a comprehensive testing program was implemented with particular attention being focused on redundancy and ductility of the structures.

For purpose of comparison, three identical beams were tested and instrumented first up to design load and in the elastic range and further loaded to ultimate capacity. These beams represented at the scale of 1 to 5 a typical 150 ft span made of a single box section 46 ft wide and 10 ft deep with match cast segments and dry joints. Although the simply supported model beams were not intended to duplicate exactly the actual continuous deck particularly insofar as tendon anchor blocks, multiple keys and loading arrangement were concerned, the test program proved very valuable.

- The first beam (bonded beam), used as a reference has the tendons inside the concrete section and grouted on their full length.

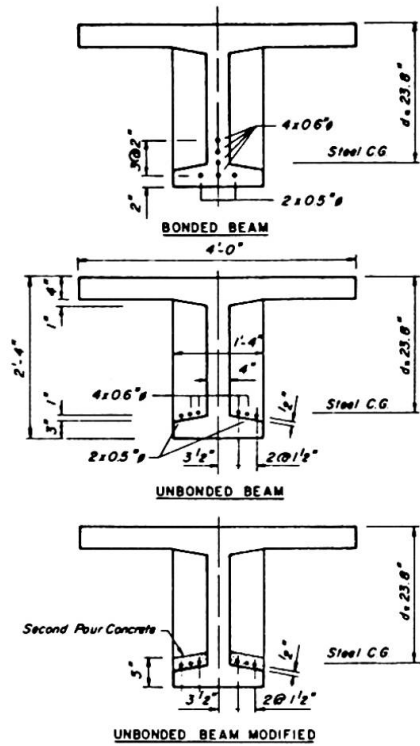
- The second beam (unbonded beam) has the tendons draped along the web but external to the concrete.

- The third beam (unbonded modified beam) was tested to ascertain the benefit of a second stage casting which would allow the tendons to be bonded to the bottom flange of the beam after stressing to sustain the applied loads.

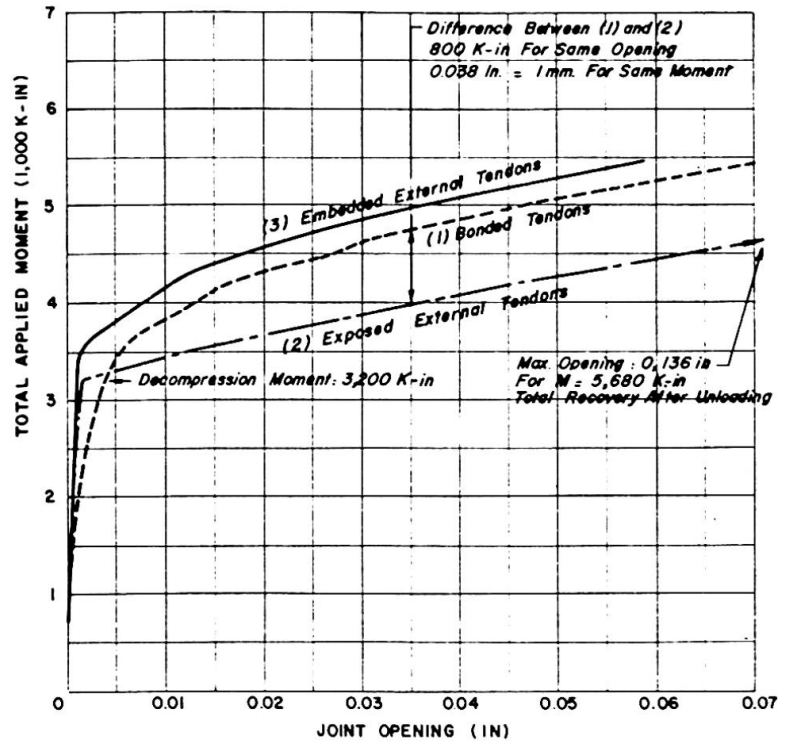
The enclosed diagrams show the relative behaviour of the three test beams and allow to draw the following conclusions: (Fig 2)

- All beams perform identically up to and including design load (load which produces the decompression of the bottom fiber at the most critical joint). For this load, the deflection at mid span was 0.3" for a 30 ft span or 1 : 1200 of the span length.

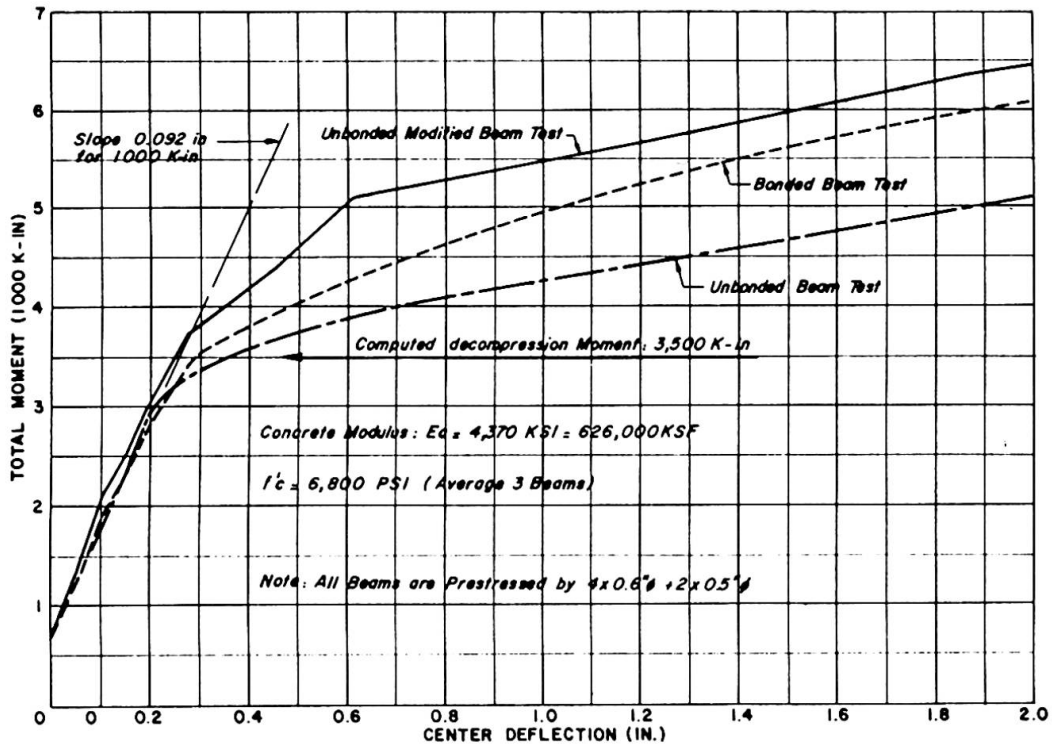




(a) DIMENSIONS OF THE THREE TEST BEAMS



(b) OPENING OF JOINT BETWEEN SEGMENTS VS TOTAL APPLIED MOMENT



(c) LOAD VS DEFLECTION CURVES

FIG. 2. COMPARATIVE BEAM TESTS.



- Beyond the design stage, the unbonded beam is the most flexible and unbonded modified beam is the most rigid. However, after reaching the state of joint opening, the slope of the moment/deflection diagram is substantially the same for three beams. This is confirmed by the diagrams of applied moment versus opening of joint between segments.

- Moreover, a complete elastic recovery was experienced after loading of the beams up to 1.7 times the design load in spite of the substantial joint opening of the critical joints (0.14 in = 3.5 mm).

- The ultimate capacity of the three beams was obtained by crushing of the top slab. The bonded beam was specifically a bending failure with strand breakage while the ultimate behaviour of the unbonded beams was influenced by the combination of maximum moment and maximum shear in the critical section (a condition never found in the actual continuous bridge deck).

- Both unbonded beams developed an ultimate moment which was the same as that of the same beam with fully bonded tendons. These experimental studies were confirmed by computer analysis.

As a conclusion, it may be stated that post tensioning by external tendons produces safe structures with the desired ductility and redundancy called for in seismically active areas. The analysis of such structures may be performed with existing design tools (computer programs). From a construction view point, external tendons are economical and easy to install. Most of the technological problems associated with tendons in the concrete (such as bursting or lamination of the concrete member and grout leakages) may be avoided while construction supervision is most simple.

## 6. CABLE STAYED BRIDGES IN THE UNITED STATES - THE SUNSHINE SKYWAY BRIDGE

Much of the experience briefly reported in the preceding paragraph was applied to the design of the new Sunshine Skyway Bridge now under construction over Tampa Bay, Florida.

Principal dimensions and design features are as follows: (see Fig 3.)

6.1. Span lengths of the main 4000 ft center unit (between expansion joints at the transition with the high level approaches)

140 - 3 x 240 - 540 - 1200 - 540 - 3 x 240 - 140 ft.

6.2. Main piers: massive foundation on drilled shafts supporting twin elliptical reinforced concrete cast in place box piers (12 x 38 ft). The individual flexibility of the piers allows for deck volume changes while the combination of twin piers affords a great bending capacity.

6.3. Pylon: single box reinforced concrete cast in place shaft.

6.4. Deck section:

- single box 95' wide 14' deep,

- deck slab and bottom slab: 8" thick web

- thickness 12" to 15" vertically prestressed

- section properties.

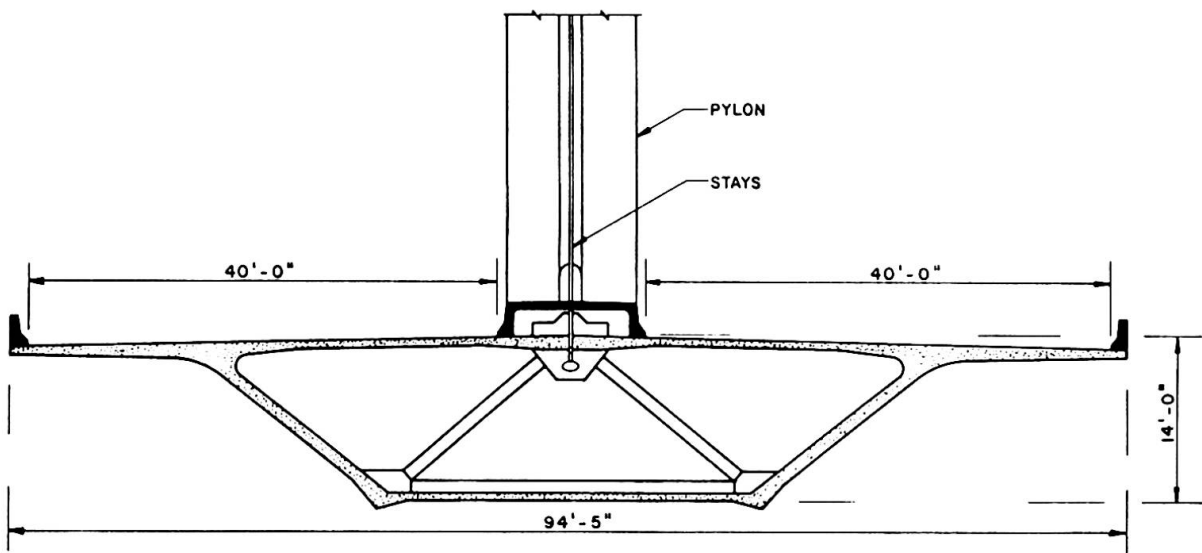
area  $A = 156$  SF

moment of inertia  $I = 4078$  ft.

6.5. Stays: single plane at bridge centerline with stays made of 60 to 80 x 0.6" strands encased in a steel pipe and pressure grouted. Stage stressing after completion of the decks includes a provision to place permanently the steel casing and the grout column under compression to minimize the effect of live load and fatigue due in particular to local bending near the anchors.



(a) RENDERING OF THE FINISHED BRIDGE



(b) TYPICAL CROSS SECTION

FIG. 3. SUNSHINE SKYWAY BRIDGE - TAMPA, Florida, U.S.A.

6.6 Stay layout: stays are placed at 24 ft intervals at deck level and a fan layout is used like in Brotonne Bridge. The angle of the stays with regard to the deck varies between 22 degrees and 47 degrees. There is a significant economy in the weight of stays afforded by the fan layout over the harp layout with all stays parallel. Also the normal load in the deck due to the component of stay loads is significantly reduced.

6.7. Construction methods: segments are fully precast and placed in balanced cantilever first in the 240 ft approach spans and then in the main span. This results in 3 closure joints for the main cable stayed structure:

- one in each transition span 420 ft from the main pier and 120 ft from the main pier and 120 ft from the transition pier,
- one at mid-span of the main crossing.

6.8. Prestressing layout: In the cable stayed span, segments are prestressed in the precasting yard in the transverse and vertical direction. In the longitudinal direction, a limited amount of prestress at top slab level allows construction in balanced cantilever before placing the first permanent stays.

The longitudinal prestress in the main span which is required to offset the combined effect of live load moments, temperature gradients and deck concrete creep and shrinkage is provided by a series of external tendons laid above the bottom slab and draped inside the box section to be successively anchored in the stay anchor block at roadway slab level in the median strip between inside barrier walls. A full continuity between stays and tendons is thus realized in the main span much in the same manner as in a suspension bridge.

## 7. BEHAVIOUR OF DECK UNDER ECCENTRIC LOADING AND ELASTIC STABILITY OF LONG SPAN CABLE STAYED BRIDGES

### 7.1. Scope

Brotonne and Sunshine Skyway Bridge decks both use a box section with a large torsional rigidity. Other schemes have been used or are contemplated where two lateral planes of stays support a relatively flexible deck (of concrete or of composite steel and concrete construction) with minimal or even negligible torsional rigidity.

It is not the intent of the author to ascertain the proper merits of the two concepts but rather to emphasize two particular points of importance pertaining to the relative behaviour of the two schemes under eccentric loading on one hand and the elastic stability of the deck on the other hand.

The comparison is simplified by using the analogy of a beam on elastic foundation.

### 7.2. Behaviour of the deck under eccentric loading

For a bridge with a single plane of stays, the torsion is entirely resisted by the concrete box section. For a bridge with two lateral plans of stays and a flexible deck, the torsion is resisted by the difference in stay loads between both planes of stays.

Taking the example of Skyway Bridge, the comparison would be the following for the effect of eccentric live loading: (three lanes on one half bridge only).

The transverse deck rotation at mid-span is:

- box and single plane of stays : 0.0040
- flexible deck and double plane: 0.0072

An exact analysis including the effect of deck moment shows infact the second bridge to have 4 times more transverse rotation than the first bridge.



### 7.3. Elastic stability of deck

The deck is subjected to high compressive stresses due to the component of the stay loads and as such liable to buckling. With the beam on elastic foundation analogy the critical buckling load would be:

$$N = 2\sqrt{kEI} \quad \left( \begin{array}{l} k \text{ spring constant} \\ EI \text{ flexural} \\ \text{rigidity} \end{array} \right)$$

and a simple derivation shows that the equivalent unsupported length for buckling is  $l = \frac{\pi a}{2}$  which is precisely half the wave length of the curves characteristic of the beam

on elastic foundation. Numerically, the comparison between the two bridges is as follows:

(unit in feet)	Box deck Single stays	Flexible deck Double stays
. Deck moment of inertia	4000	300
. Radius of gyration	5.10	1.53
. Characteristic length	192	99
. Unsupported length	300	155
. Slenderness ratio	<u>59</u>	<u>101</u>

The increased rigidity of the box section is evident and this is particularly important in the case where one stay would be accidentally lost (derailment, accident or fire for example).

### 8. RECENT DEVELOPMENTS IN MODERATE SPANS

Essentially used for long spans (in excess of 800 ft) where box girder bridges are no more competitive due to their rapidly increasing weight, the cable stayed concept proves now its merits for shorter span lengths (in the range of 500 to 700 ft). This was recently confirmed by the results of the bidding of the Neches River Bridge in Texas with a 640 ft. main clear span. An alternate design with a concrete cable stayed box girder deck proved to be the most economical scheme over all other conventional steel or concrete solutions.

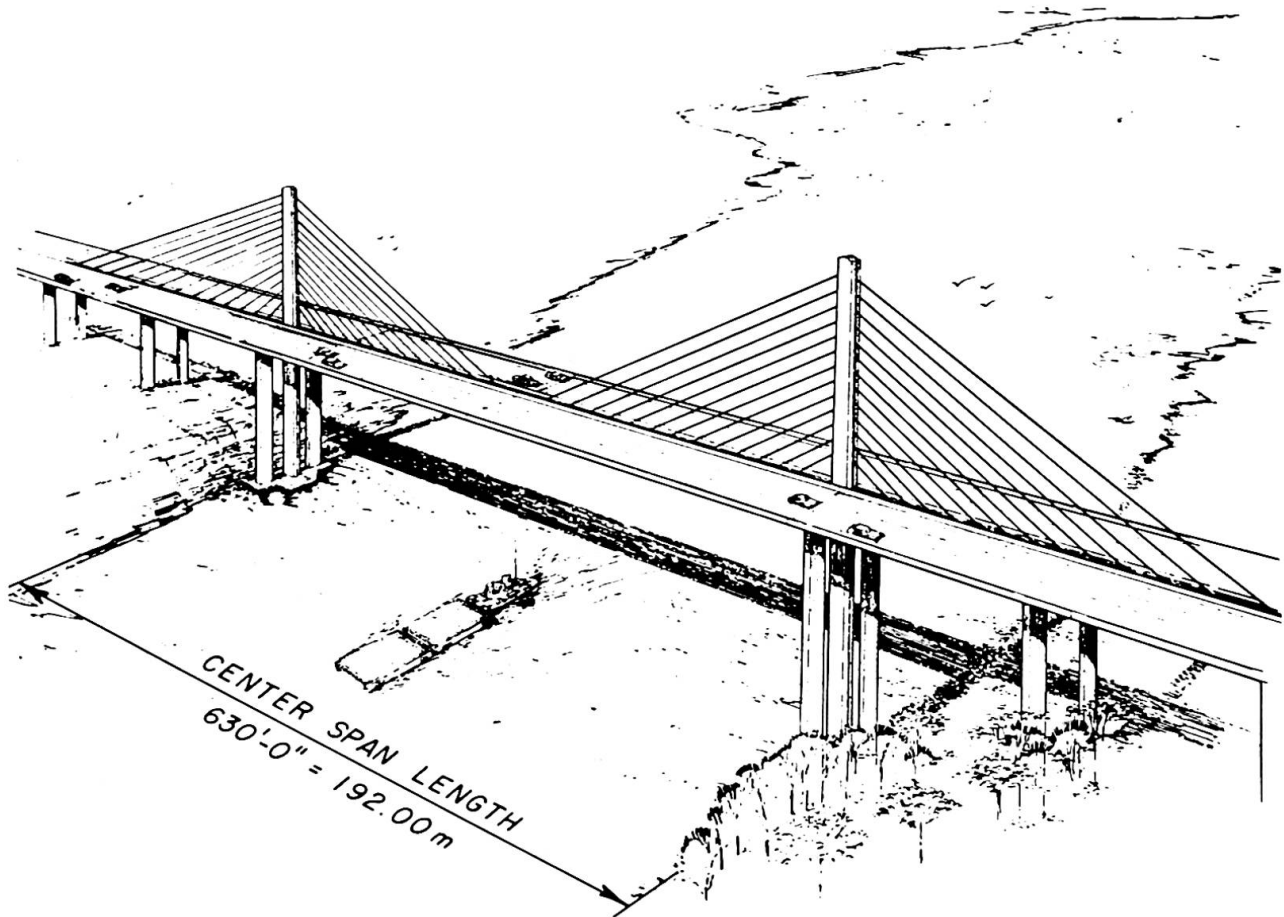
Similar conclusions were reached for other projects such as the Cooper River Bridge in South Carolina or the James River Bridge project in Virginia during the design stage after careful cost studies.

Probably the key reason for this trend is the use of new simplified design concept and construction process.

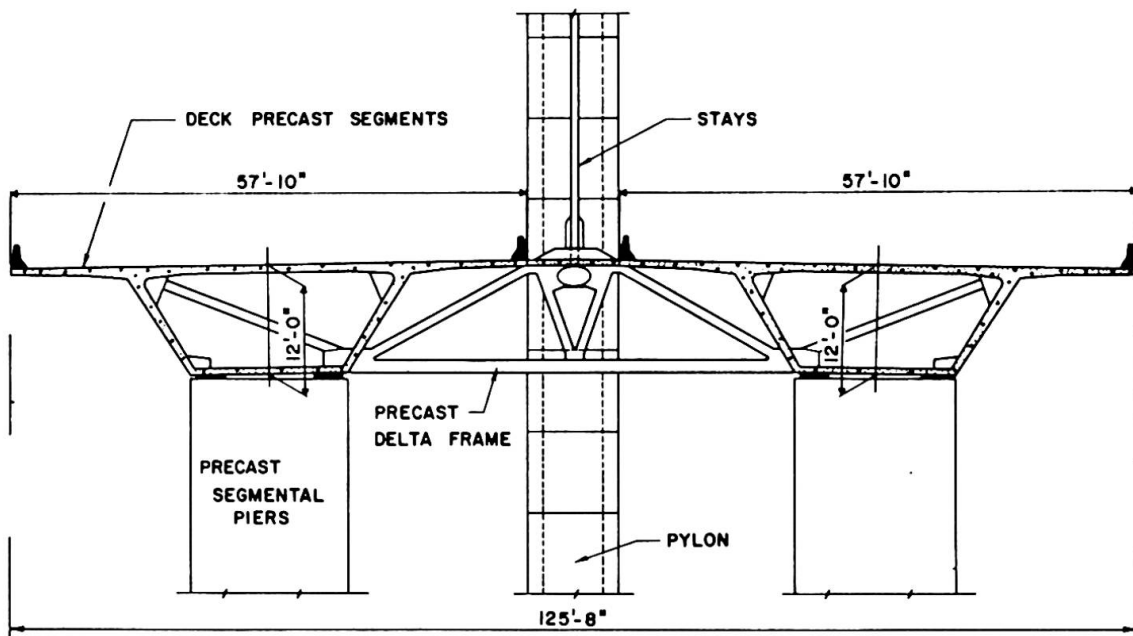
The main span is now considered as a natural continuation of the approach spans both for the choice of deck cross section and for the method of constructing the deck.

In the frequent case of twin structures each carrying 2 or 3 traffic lanes for width of 35 to 55 ft., the approach spans are conveniently built with two separate parallel box girders of constant depth. Precast segmental with span by span construction has proven well suited to that type of project.

The same structure may in fact be used to construct the main cable stayed span (see Fig. 4 the example of James River Bridge). A series of transverse frames located at the section where the stays are anchored into the deck will allow the loads of both box girders to be transferred to the center plane of suspension. This scheme requires less quantities of materials than the equivalent single deck on the full width. The investment in special equipment is also significantly reduced.



(a) ISOMETRIC VIEW OF THE FINISHED BRIDGE



(b) TYPICAL CROSS SECTION

FIG. 4. JAMES RIVER BRIDGE PROJECT, VIRGINIA



The erection scheme becomes now very simple: the transition spans up to the main piers are constructed in the same fashion as the approach spans. The main span proceeds thereafter in one directional cantilever towards the center while stays and transverse frames are installed at each step of construction.

This concept is believed to be competitive over conventional girder designs for spans as short as 400 ft.

## 9. CONCLUSIONS

Primarily used initially for long spans, the cable stayed concept will certainly find in the near future many applications in shorter spans.

With present materials properties (concrete and steel) a 2000 ft. clear span can be built entirely in concrete. Beyond this point, steel or an association of concrete and steel should be more economical.

In the range of very short spans, pedestrian bridges have already been built with a cable stayed deck. Recently, Professor Walther of Lausanne has prepared a design for a cable stayed highway bridge in Switzerland with a main span of only 97m. (318 ft). The deck is a solid slab with a maximum thickness of 0.55m (22 inches) supported on each side by a series of stays anchored over an H framed pylon. The bridge is now under construction (1984). The deck is cast in place on a very simple and inexpensive travelling formwork.

In both fields of very long spans and of short spans, the future of cable stayed bridges looks bright.

Progress will undoubtedly take place as more experience is gained in the following areas:

- choice of static scheme (proportions of flanking spans, number and position of intermediate piers, connection between deck and pylon).
- proper association of steel and concrete for composite designs.

Logical in its concept, the cable stayed structure has already acquired an excellent record of performance.

With simple and functional shapes, the structure may be given the added touch of an aesthetically pleasing work of art.

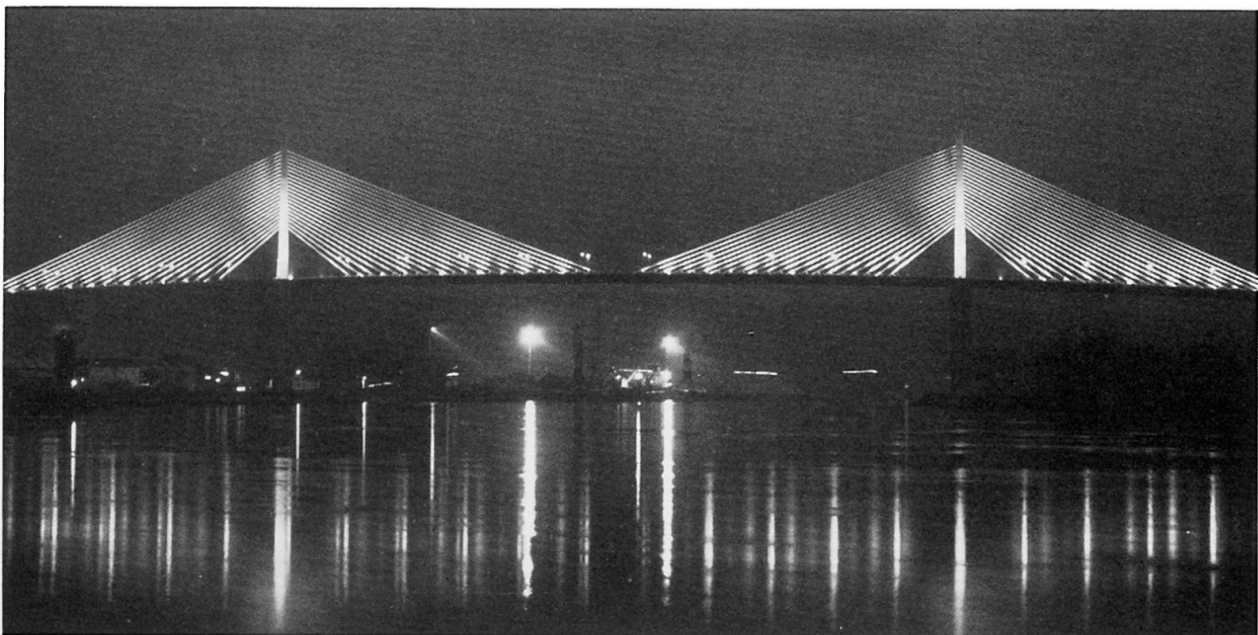


FIG. 5 BROTONNE BRIDGE BY NIGHT

## Damage and Risk Considerations for Selecting Seismic Design Requirements

Réflexions sur les risques et les dommages pour le choix des prescriptions sismiques

Betrachtungen über Schaden und Risiko zur Wahl von Erdbebenbemessungsanforderungen

### Luis ESTEVA

Director  
Inst. of Eng., Nat. Univ.  
Mexico City, Mexico



Luis Esteva, born 1935, got his civil engineering and doctor degrees from the National University of Mexico and a master degree from the Massachusetts Institute of Technology. He has been involved in research and consulting in earthquake engineering and structural safety since his graduation.

### SUMMARY

This paper discusses some problems related with the determination of the failure probability of structural systems with uncertain properties subjected to random earthquake histories. The main purpose is to show how the relation between the expected failure rate of a structural system and the rate of occurrence of earthquakes with intensities greater than the design value is affected by variables such as uncertainty about system properties,  $P-\Delta$  effects, number of potential failure modes and safety factors with respect to brittle and ductile failure modes.

### RESUME

Cette communication traite de certains problèmes liés à la détermination de la probabilité de rupture de systèmes structuraux à propriétés incertaines et soumis à une succession aléatoire de séismes. Son objectif principal est de déterminer l'influence de facteurs tels que l'incertitude sur les propriétés du système, les effets  $P-\Delta$ , le nombre de modes de rupture potentiels et les facteurs de sécurité face aux modes de rupture fragile et ductile, sur la relation entre l'espérance de vie d'un système structural et le nombre de séismes dont l'intensité est supérieure à l'intensité de projet.

### ZUSAMMENFASSUNG

Dieser Artikel behandelt einige Probleme der Bestimmung der Ausfallwahrscheinlichkeit von Bauwerken, die durch Erdbeben beansprucht werden. Im Speziellen befasst sich der Artikel mit der Beziehung zwischen der erwarteten Versagenswahrscheinlichkeit des Bauwerkes oder eines Teils desselben und der Eintretenswahrscheinlichkeit von Erdbeben, deren Intensität grösser als die Intensität des der Bemessung zugrunde gelegten Bebens ist. Diese Betrachtungen berücksichtigen Unsicherheiten der Eigenschaften des Bauwerkes,  $P-\Delta$  Effekte, Anzahl mögliche Versagensarten und Sicherheitsfaktoren im Hinblick auf sprödes oder elastisches Versagen.





## 1. INTRODUCTION

The main purpose of this paper is discussing a link which is missing in conventional seismic risk studies.

Significant research efforts have been devoted during the last few years to problems such as the probabilistic analysis of seismic hazard, the establishment of reliability based criteria for structural design and the development of cost-benefit and risk-cost-benefit criteria and methods for selecting optimum design values and safety factors. The results of this research have enabled structural engineers to produce designs for which the values of safety factors and failure probabilities for different critical members, sections or modes are such that the degrees of protection that each design is expected to provide with respect to the different potential failure modes are consistent with the corresponding expected costs, both those due to initial construction and those which may arise from failure and damage. In other words, the present development of the theory of probabilistic structural safety has permitted the establishment of adequate ratios, or relative values, of the mentioned safety factors or failure probabilities. However, if we talk about the absolute values of those variables we must recognize that neither the optimum safety levels nor the corresponding safety factors and design parameters have been derived for specific practical cases on the sole basis of the probabilistic theory of structural reliability: when reaching the point of stating desirable safety factors or  $\beta$ -values we resort to calibration with conventional design practice.

The probabilistic theory of structural safety has enabled code writers to decide which structure should be safer than other, and how safer, and therefore to make statements about the relative values that should be adopted for the corresponding safety factors; but establishing the desirable absolute values of those factors is something that has not escaped a comparison with or an adjustment to values that engineers have semi-intuitively arrived at after many years of trial and error. And those who try to make quantitative studies about the relations between the return periods of earthquake intensities adopted for design, the implicit failure probabilities and the observed failure rates bewilder at the numerous hindrances and apparent discrepancies; and yet, an extremely small amount of research efforts has been oriented to overcoming those hindrances and understanding those discrepancies.

For very important structures, such as large dams, large efforts and bitter arguments are spent in the establishment of seismic hazard curves (intensities vs return periods), and also in deciding what return period should be considered as the basis of design specifications. Nevertheless, the last link in the chain is overlooked: in general no attention is paid to a quantitative analysis of the influence that on failure probabilities have the probability density functions of the structural parameters and of the relationship between nominal design values, mean values and dispersion measures of those parameters. As a consequence, no clear understanding has been reached of the ratio of expected failure rates of given systems to rates of exceedence of design intensities. The need to understand this relation motivated the studies described herein.

What are the main reasons for the engineering profession and the participants in seismic-risk-related decisions to have overlooked this missing link? We can mention at least the following: the difficulties attached to handling of uncertainties associated with modelling of seismic hazard, the complexities involved in obtaining failure probabilities of systems with uncertain properties subjected to random earthquake excitation and the difficulties that arise when trying to evaluate failure consequences as well as when trying to express consequences of different types in the same scale, in order to build utility (objective) functions to be optimized. This paper is centered on the second of the above points -which does not mean that the other two are not at least equally relevant and worthy of study.

In the following, a very brief review will be presented of the basic concepts related to descriptions of seismic hazard and risk and their application to decision making. Then the influence of uncertain structural parameters and seismic design criteria on seismic reliability will be discussed in detail.

## 2. SEISMIC HAZARD AND SEISMIC RISK

Seismic hazard relates to the likelihood of occurrence of earthquakes of different sizes and intensities at given sources, regions or sites. In quantitative terms, it can be expressed by joint probability distributions of magnitudes, intensities, times of occurrence and locations of seismic events. Seismic risk involves the likelihood of different degrees of damage. Typical (but not necessarily complete) descriptors of it are failure probabilities for given intensities or for given time intervals, probability distributions of time to failure, expected failure rates or expected costs of damage per unit time. Significant progress has been lately attained in the development of relatively sophisticated stochastic process models of seismic hazard [1-4] but their use for the development of seismic risk descriptors other than expected failure rates or expected costs of damage -which suffice as descriptors of risk when seismic activity is modelled as a homogeneous Poisson process with stochastically independent selection of intensity- is virtually unexplored.

If the seismic resistance of a structural system can be deterministically measured by the earthquake intensity causing the system to fail, the failure rate,  $v_F$ , is equal to the rate of occurrence of earthquakes having intensities  $Y$  greater than the resistance,  $y^*$ . For many applications the latter rate can be expressed as  $v(Y) = KY^{-r}$  [5], where  $K$  and  $r$  are site dependent parameters and  $y^*$  should be substituted for  $Y$ . Under the assumptions that the system can only remain in the zero-damage state or suffer total collapse, that any time that the latter state is reached the system is instantaneously rebuilt in accordance with the same specifications, the present value of the expected cost of failure is equal to  $D = D_0 v_F / \gamma$  [1, 6], where  $D$  is the cost of each failure and  $\gamma$  is the applicable discount rate (that is, a number such that a given cost or benefit  $U_1$  suffered or perceived at instant  $t$  is equivalent to a utility  $U = U_1 \exp(-\gamma t)$  at instant  $t = 0$ ).

The seismic strength of a real structure to be built in accordance with a given design is not deterministically known in advance. The uncertainty is made up from the contributions of that associated to the material properties and of the randomness in the detailed ground motion characteristics for a given intensity. To these must be added the systematic or random errors arising from the inaccuracies of the structural response analysis algorithms. In ref. 1 these uncertainties are grouped according to whether they can be handled in terms of random variables independent from some seismic event to the other (denoted as type 1 uncertainty) or as dependent on the properties of the structural system, and changing only every time that the system is rebuilt (type 2 uncertainty). The same reference deals with the case when earthquakes take place in accordance with a Poisson process with mean rate of occurrence  $v_0$  and random selection of intensities and of variables of type 1, and the structural properties are uncertain. If the system is repaired every time it is damaged so as to return it to its previous state, and in case of collapse it is replaced with a system (with uncertain properties) built in accordance with the same specifications as the original one -and therefore with the same distribution of structural properties- the present value of the expected cost of failure and damage is shown to be  $D$  as given by the following equation:

$$D = \frac{E_2 \left[ \left( A_C + \frac{A_d}{P} \right) \mu \right]}{1 - E_2(\mu)} \quad (1)$$



Here,  $\mu = v_0 P / (\gamma + v_0 P)$ ,  $A_c$ ,  $v_0$  and  $\gamma$  were defined above,  $E_2(\cdot)$  is an expected value taken with respect to the probability density function of the variables in group 2, and  $P$  and  $A_d$  are respectively the failure probability and the expected cost of damage other than collapse of a deterministic system for each earthquake of random intensity. The latter quantity is computed as follows

$$A_d = \int_0^R \delta(u/R) f_Y(u) du \quad (2)$$

In this equation,  $\delta$  is a damage function which depends on the ratio of earthquake intensity to structural strength  $R$ , and  $f_Y$  is the probability density function of earthquake intensities.

When the uncertainties associated to the variables of group 2 are not too large, eq. 1 may be approximated with the following

$$D \cong E_2 \left[ \left( A_c + \frac{A_d}{P} \right) \frac{v_0 P}{\gamma} \right] \quad (3)$$

An important part of this paper is devoted to assessing the influence of uncertainty about system properties on  $E_2(v_0 P)$  -the expected failure rate- and its relation to  $v^*$  - the rate of occurrence of earthquakes with intensities greater than the design value.

### 3. INTENSITY, RESPONSE AND FAILURE CONDITION

Fig. 1 shows a set of linear response pseudovelocity spectra for the El Centro earthquake of 1940 on a four-log plot, which also shows peak values of ground acceleration, velocity and displacement ( $a$ ,  $v$ ,  $d$ ). The ordinates of the pseudovelocity spectra are assumed to be the sum of the expected values shown by the dashed lines, which are determined by  $a$ ,  $v$  and  $d$ , and random deviations with respect to the expected value. The latter can be obtained from  $a$  and  $d$  as follows

$$\frac{\bar{S}_v}{\sqrt{ad}} = \frac{\chi}{[(1 - \chi^m + e\chi^{m/z})^{zn} + D(\chi)]^{1/mn}} \quad (4)$$

Here,  $\chi = \omega/\omega_0$ ,  $\omega$  is natural frequency,  $\omega_0 = \sqrt{a/d}$ ,  $e = 0.15$ ,  $m = 0.5$ ,  $n = 2$  and  $D(\chi) = \alpha_1 \chi^{0.7} + \alpha_2 \chi^2$ , where  $\alpha_1$  and  $\alpha_2$  are functions of the damping ratio. If the second member in eq. 4 is denoted by  $G(\chi)$ , the linear response spectra of other earthquakes can be scaled with respect to  $a$  and  $v$  as follows

$$\frac{\bar{S}_v}{a} = G(\chi) \frac{v}{a} \frac{\sqrt{ad}}{v} \quad (5a) \quad , \quad \frac{\bar{S}_v}{v} = G(\chi) \frac{\sqrt{ad}}{v} \quad (5b)$$

Using information available for the earthquake record being considered, simple equations have been obtained for the ordinates of the elastoplastic displacement spectra  $D$ , in terms of the yield ratio  $\epsilon_y = A_D \bar{S}_d^{-1} \omega^{-2}$ , where  $A_D$  is the ratio of lateral strength to vertical load expressed in units of gravity and  $\bar{S}_d$  is the expected linear displacement spectrum, equal to  $\bar{S}_v \omega^{-1}$ . The results can be expressed as

$$D = \bar{S}_d \frac{Q + 8TQ}{1 + 8TQ} \xi_{De} \quad (6)$$

where  $Q$  is the required ductility factor,  $T$  is the natural period (equal to  $2\pi/\omega$ ) and  $\xi_{De}$  is an uncertainty factor which depends on  $T$  and  $Q$ .

The failure condition for a simple elastoplastic system is obtained by equating response and deformation capacity, that is

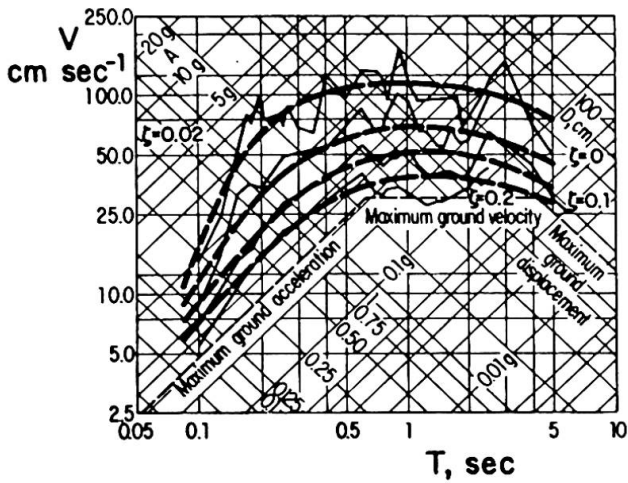


Fig. 1 Linear response spectra. El Centro, 1940

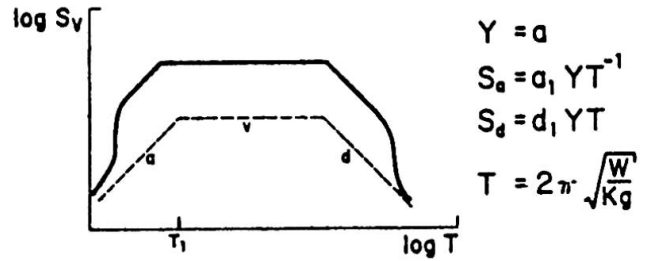


Fig. 2 Simplified expected spectrum

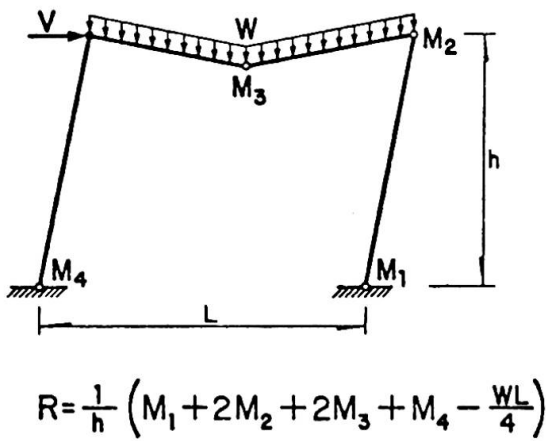


Fig. 3 Lateral resistance of single-story structure

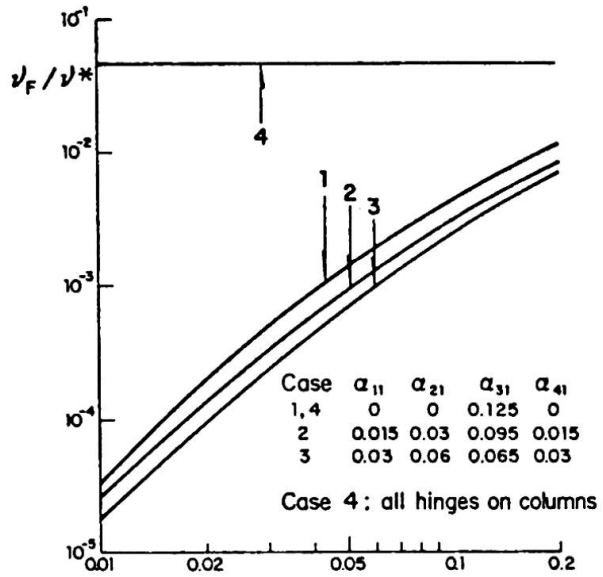


Fig. 4 Failure rates for single-story frames

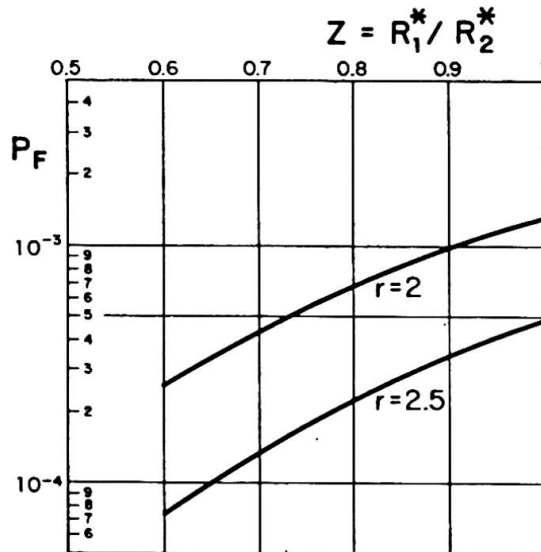


Fig. 5 Simple systems with ductile and brittle failure modes

$$v_G(\chi) \frac{\sqrt{ad}}{v} \cdot \frac{1}{\omega} \frac{Q + 8TQ}{1 + 8TQ} \xi_{De} = QR/K \quad (7)$$

where  $K$  is lateral stiffness and  $R$  is lateral strength. The probability of failure is the probability that the first member is greater than the second. The failure intensity  $v$  can be obtained solving for  $v$  in eq. 7. The first two moments of its probability density function can then be obtained by straight forward application of first-order second-moment analysis (7).

A simplified condition is used in the following for the purpose of making a parametric study of the expected failure rates of simple and multi-story elastoplastic building frames: instead of adopting for  $G(\chi)$  the form defined by eq. 4 and depicted in fig. 1, use is made of the conventional form shown in fig. 2, under the assumptions that intensity is measured by peak ground acceleration  $a$  and that the natural periods of all systems studied lie well within the constant pseudovelocity branch. Linear spectral acceleration and displacement are related to  $Y$  in accordance with the expressions shown in fig. 2, where  $a_1$  and  $d_1$  are transformation coefficients. Thus, instead of eq. 7 the following failure condition is obtained,

$$Y d_1 (2\pi \sqrt{\frac{w}{Kg}}) \xi_{De} = \frac{QR}{K} \quad (8)$$

and the ratio of the random failure intensity  $Y$  to its nominal design value  $Y^*$  equals

$$\frac{Y}{Y^*} = \frac{\sqrt{k^* w^*}}{q^* \rho^*} \frac{q\rho}{\xi_{De} \sqrt{kw}} \quad (9)$$

where  $k = K/\bar{K}$ ,  $k^* = K^*/\bar{K}$ ,  $q = Q/\bar{Q}$ ,  $q^* = Q^*/\bar{Q}$ ,  $\rho = R/\bar{R}$ ,  $\rho^* = R^*/\bar{R}$ ,  $w = W/\bar{W}$ ,  $w^* = W^*/\bar{W}$ ; the asterisks denote nominal design values and the bars denote mean values.

#### 4. EXPECTED FAILURE RATES

Under the assumptions that  $Y$  in eq. 9 has a lognormal distribution and that  $v(y) = Ky^{-r}$ , the expected failure rate  $v_F$  and the rate of exceedence of the design intensity,  $v^*$ , are related as follows

$$\frac{v_F}{v^*} = \left(\frac{Y^*}{\bar{Y}}\right) (1 + V_Y^2) \frac{r(r-1)}{2} \quad (10)$$

Here,  $\bar{Y}$  and  $V_Y$  are mean value and variation coefficient of  $Y$ , and  $Y^*$  is the nominal value of the design intensity. If  $Y^*$  is related to  $\bar{Y}$  through the expression  $Y^* = \bar{Y} \exp(-2V_Y)$  [8], one obtains that  $v_F/v^*$  equals 0.26 and 0.15 if  $r$  equals respectively 2.5 and 4 and  $V_Y = 0.3$ .

In order to study the variation of  $v_F/v^*$  for the most frequent ranges of values of  $Y^*/\bar{Y}$  and  $V_Y$ , a parametric study was carried out for a single-story frame depicted in fig. 3 in its yielding mechanism. The lateral strength  $R$  is as shown in the same figure. The vertical load  $W$  and the resisting moments  $M_i$  at critical sections were considered as random variables. The nominal design values of those moments are  $M_i^* = \psi W^* L (\alpha_{i1} + \alpha_{i2} \epsilon)$ , where  $\epsilon = V^* h / (W^* L)$ ,  $\psi$  is a load factor (taken here as 1.1, in accordance with Mexico City seismic code),  $\alpha_{i1}$  and  $\alpha_{i2}$  are influence coefficients for vertical and lateral load respectively and  $V^*$  is nominal value of design lateral load. Fig. 4 shows the results in terms of  $\epsilon$  for the sets of values of  $\alpha_{i1}$  listed in the same figure and the following values of the other parameters:  $\alpha_{12} = \alpha_{42} = 0.3$ ,  $\alpha_{22} = 0.2$ ,  $\alpha_{32} = 0$ ,  $h/L = 0.5$ ,  $V_W = 0.25$ ,  $w^* = 1.65$ ,  $V_{M_1} = 0.25$ ,  $m_1^* = 0.61$ ,  $\rho_{ij} = \delta_{ij} + 0.25(1 - \delta_{ij})$ ,  $V_K = 0.15$ ,  $k^* = 0.74$ ,  $V_Q = 0.3$ ,  $q^* = 0.55$ ,  $\xi = 1$ ,  $V_\xi = 0.25$ . Here,  $V$  means variation coefficient,  $m_1^* = M_1^*/\bar{M}$ , and  $\rho_{ij}$  is the correlation coefficient between  $M_i$  and  $M_j$ .

Curves 1, 2 and 3 in fig. 4 show a strong dependence (orders of magnitude) of  $v_F/v^*$  on the ratio of the nominal design shear force to the design vertical load. This is due to the lateral strength which results from continuity considerations when designing for vertical load. A constant value is obtained for case 4, which assumes that the yielding mechanism is produced by hinges at the column ends and that  $\alpha_{i1} = 0$  for all  $i$ . This constant value is an upper bound to the other curves.

An approximate analysis was carried out in order to study the possible influence of multiple, imperfectly correlated, failure mechanisms, on the reliability of a multistory system, as compared to that of a simple system. Shear buildings having 1, 2, 5, 10 and 20 stories were studied. They were assumed to have been designed so as to provide uniform safety factors for all story shears. The objective was to obtain the first two moments of the probability density function of the ratio of the failure intensity (that is, of the minimum of the failure intensities  $Y_i$  determined for the individual stories) to the design value. This was achieved by means of a Monte Carlo approach, using the following parameters

$q^* = 0.53$	$V_Q = 0.3$	$\rho_{ij} = 0.5$	$q, r$ and $\xi$ mutually independent
$r^* = 0.72$	$V_R = 0.2$	$\rho_{ij} = 0.5$	
$\xi^* = 1$	$V_\xi = 0.25$	$\rho_{ij} = 0.5$	$v = Ky^{-r}, r = 2.5$
$k^* = 0.74$	$V_k = 0.15$	$\rho_{ij} = 1$	
$w^* = 1.65$	$V_w = 0.25$	$\rho_{ij} = 1$	$\psi = 1.1$

The results are summarized in the following table, where  $\lambda = \min(\ln(Y_i/Y^*))$  and  $y_n^*/y_1^*$  is the ratio of the design intensity for  $n$  stories to that for 1 story required for obtaining equal failure rates. The last two columns are obtained under the assumption that  $\lambda$  has a lognormal distribution.

$n$	$\bar{\lambda}$	$\text{var } \lambda$	$y_n^*/y_1^*$	$y_n^*/y^*$
1	1.11	0.21	0.055	1.0
2	0.96	0.17	0.082	1.17
5	0.79	0.15	0.126	1.40
10	0.69	0.14	0.165	1.55
20	0.56	0.14	0.228	1.77

The influence of multiple failure modes is obvious.

##### 5. SLENDERNESS EFFECTS (P- $\Delta$ )

Ref. 9 presents a plot of the failure probabilities of deterministic simple bi-linear hysteretic systems subjected to segments of duration 15 sec of stationary Gaussian white noise. Each system is determined by its initial stiffness  $K_1$ , the negative stiffness  $K_2 = -W/H$  of the second portion of the force-deflection curve, the damping ratio  $\zeta = 0.03$  and the yield deflection  $y_0$ , equal to 0.25 times the expected maximum linear response displacement. The table that follows summarizes failure probabilities obtained from fig. 8 of ref. 9

T	$K_1/ K_2 $			
	100	80	40	20
0.8	$1.13 \times 10^{-4}$	$3.30 \times 10^{-3}$	0.157	0.555
1	$7.31 \times 10^{-5}$	$2.33 \times 10^{-3}$	0.114	0.479
1.5	$4.54 \times 10^{-5}$	$1.10 \times 10^{-3}$	0.082	0.368
2	$4.54 \times 10^{-5}$	$1.01 \times 10^{-3}$	0.062	0.287
2.5	$4.54 \times 10^{-5}$	$1.01 \times 10^{-3}$	0.040	0.230
3	$4.54 \times 10^{-5}$	$1.01 \times 10^{-3}$	0.036	0.199
3.5	$4.54 \times 10^{-5}$	$1.01 \times 10^{-3}$	0.032	0.184
4	$4.54 \times 10^{-5}$	$1.01 \times 10^{-3}$	0.028	0.168

This table shows that, as  $K_1/|K_2|$  and the natural period increase, the failure probability decreases, and that beyond a given period the failure probability remains constant. Values of  $K_1/|K_2|$  of about 20 are not infrequent in practical cases.

The above results were used to obtain estimates of failure probabilities of deterministic multistory buildings including P- $\Delta$  effects. It was assumed that the dynamic response is the product of a function of time by the shape of the fundamental mode, and that P- $\Delta$  effects give place to reduced lateral stiffness but do not affect the shape function; in other words, the response of the multistory systems was obtained from that of a simple system by assuming the generalized mass and initial stiffness valid for a linear modal analysis, and extending the concept of generalized stiffness to the range of negative stiffness values. It was also assumed that the fundamental natural period T in seconds varies as H/30 where H is the building height in meters. A summary of the results follows. The last column shows the ratio of the design intensities required to give place to the failure probability corresponding to a system with T = 1 sec

T	$P_F$	$y_0(T)/y_0(1)$
1.0	$1.93 \times 10^{-3}$	1.0
1.5	$1.98 \times 10^{-2}$	1.25
2.0	$6.22 \times 10^{-2}$	1.58
2.5	$9.25 \times 10^{-2}$	1.76
3.0	$1.46 \times 10^{-1}$	1.92
3.5	$1.62 \times 10^{-1}$	2.12
4.0	$1.68 \times 10^{-1}$	2.22

## 6. SAFETY WITH RESPECT TO DUCTILE AND BRITTLE FAILURE MODES

Let  $R_1$  be the lateral force required to make a simple system reach its yield strength in a ductile failure mode and  $R_2$  the lateral force required to make that system reach its maximum capacity with respect to a perfectly brittle failure mode. The system fails in a ductile manner if the internal force  $S_1$  giving place to ductile failure is reached before the internal force  $S_2$  giving place to brittle failure. If this happens,  $S_2$  is controlled by the facts that it is correlated with  $S_1$  and that the latter cannot grow above the value that gives place to ductile failure. This can be expressed by the condition that  $S_2 \leq \gamma_{21} R_1$ , where  $\gamma_{21}$  is random. If the design value  $R_2^*$  with respect to the brittle mechanism is kept constant and the design value  $R_1^*$  with respect to the ductile mode is made to grow, one does not obtain a safer structure, but one for which the probability of reaching the brittle failure condition is greater. This is shown in fig. 5 for a set of values of the relevant parameters which are representative of usual practical cases. the probability of failure corresponds to the occurrence of one earthquake of random intensity for two cases of the parameter r in the equation  $v = Ky^{-r}$ .

## 7. CONCLUSIONS

An analysis has been presented of the influence of the uncertainty about structural parameters as well as of design criteria on the expected failure rates of structures subjected to earthquakes. On the basis of approximate estimates of the probabilistic dynamic response, the following can be concluded:

- Failure rates of structures with uncertain parameters may be orders of magnitude smaller than rates of occurrence of earthquakes with intensities greater than the design values.
- A very important variable contributing to this difference is, as should have been expected, the lateral strength already available in continuous frame

structures subjected to vertical loads.

- c) Due to the possible occurrence of multiple failure modes, multistory buildings may be less safe --and significantly so-- than single-story structures nominally designed for the same spectrum and the same safety factors.
- d) Accounting for  $P-\Delta$  effects may drastically affect failure probabilities, even in ranges of parameters usual in real structures. The influence of these is very sensitive to the natural period. This is true also for multistory systems.
- e) Overdesign with respect to ductile failure modes may be harmful, rather than beneficial, if safety factors with respect to brittle modes are not correspondingly raised. The results shown are based on crude estimates of the probabilistic dynamic response of nonlinear systems. In view of the very high sensitivity of failure probabilities to the variables studied, more detailed studies along the same lines, but using more refined models, are strongly recommended.

#### REFERENCES

1. ROSENBLUETH, E., Optimum design for infrequent disturbances, Journal of the Structural Division, Proc. ASCE, Vol. 102, No. ST9, September 1976.
2. VERE JONES, D., Stochastic models for earthquake occurrences, Journal of the Royal Statistical Society, Vol. 32, p.1-62, 1970.
3. VERE JONES, D., Stochastic models for earthquake sequences, Geophysical Journal of the Royal Astronomical Society, Vol. 21, p. 323-335, 1975.
4. KNOPOFF, L., A stochastic model for the occurrence of main-sequence earthquakes, Reviews of Geophysics and Space Physics, Vol. 9, No. 1, 1971.
5. ESTEVA, L., Seismicity, Chapter 6 of the book Seismic risk and engineering decisions, edited by C. Lomnitz and E. Rosenblueth, Elsevier, Amsterdam, 1976.
6. ESTEVA, L., Seismic risk and seismic design decision, Seminar on seismic design of nuclear power plants, MIT Press, Cambridge, Mass., 1970.
7. BENJAMIN, R.R. and CORNELL, C.A., Probability, statistics and decisions for civil engineers, McGraw-Hill Book Company, New York, 1970.
8. ROSENBLUETH, E. and ESTEVA, L., Reliability basis for some Mexican codes, included in ACI Special Publication 31, Detroit, 1971.
9. VENEZIANO, D., Analysis and design of hysteretic structures for probabilistic seismic resistance, Proc. Fourth World Conference on Earthquake Engineering, Rome, 1973.



Leere Seite  
Blank page  
Page vide